Tellus SERIES B CHEMICAL AND PHYSICAL METEOROLOGY
PUBLISHED BY THE INTERNATIONAL METEOROLOGICAL INSTITUTE IN STOCKHOLM

Large variability in ecosystem models explains uncertainty in a critical parameter for quantifying GPP with carbonyl sulphide

By TIMOTHY W. HILTON[1]*, ANDREW ZUMKEHR[1], SARIKA KULKARNI[2,3], JOE BERRY[4], MARY E. WHELAN[1] and J. ELLIOTT CAMPBELL[1], [1]*Sierra Nevada Research Institute, University of California, Merced, CA, USA;* [2]*Center for Global and Regional Environmental Research, University of Iowa, Iowa City, IA, USA;* [3]*California Air Resource Board, Sacramento, CA, USA;* [4]*Department of Global Ecology, Carnegie Institution, Stanford, CA, USA*

(Manuscript received 16 October 2014; in final form 29 June 2015)

ABSTRACT

Regional gross primary productivity (GPP) estimates are crucial to estimating carbon-climate feedbacks but are highly uncertain with existing methods. An emerging approach uses atmospheric carbonyl sulphide (COS) as a tracer for carbon dioxide: COS plant uptake is simulated by scaling GPP. A critical parameter for this method is leaf-scale relative uptake (LRU). Plant chamber and eddy covariance studies find a narrow range of LRU values but some atmospheric modelling studies assign values well outside this range. Here we study this discrepancy by conducting new regional chemical transport simulations for North America using the underlying data from previous studies. We find the wide range of ecosystem model GPP estimates can explain the discrepancy in LRU values. We also find that COS concentration uncertainty is more sensitive to GPP uncertainty than to LRU parameter uncertainty. These results support the COS tracer technique as a useful approach for constraining GPP estimates.

Keywords: carbon cycle, GPP, carbonyl sulphide

1. Introduction

Understanding gross primary productivity (GPP) is of great importance for forecasting climate change due to the large magnitude and uncertainty of terrestrial carbon-climate feedbacks (Arneth et al., 2010). Much of this uncertainty stems from ecosystem models' wide inconsistencies with respect to GPP simulations (Friedlingstein et al., 2006, 2014; Huntzinger et al., 2012; Fisher et al., 2014). Reducing GPP uncertainty is challenging because we lack robust tools for measuring GPP at regional and global scales. Large-scale observations of atmospheric CO_2 (e.g. tall tower and airborne measurements) alone may not be useful for constraining GPP because they are simultaneously influenced by both GPP and respiration. Finding new observation-based methods to constrain GPP represents a critical scientific need that may be addressed through emerging methods with atmospheric carbonyl sulphide (COS) analysis (Montzka et al., 2007; Campbell et al., 2008), eddy flux measurements (Beer et al., 2010), oxygen isotopes (Welp et al., 2011) and fluorescence (Guanter et al., 2014).

A global network of surface and airborne observations COS observations (Montzka et al., 2007), airborne intensive campaigns (Blake et al., 2004; Campbell et al., 2008), remote sensing (Kuai et al., 2014) and breakthroughs in instrumentation have motivated new atmospheric COS studies that aim to investigate GPP at multiple spatial and temporal scales (Montzka et al., 2007; Campbell et al., 2008; Stimler et al., 2010; Blonquist et al., 2011; Asaf et al., 2013; Berry et al., 2013; Commane et al., 2013; Berkelhammer et al., 2014; Billesbach et al., 2014; Kuai et al., 2014). The COS tracer approach is based on the condition that there is a well-constrained relationship between plant uptake of COS and the GPP uptake of CO_2:

$$F_{plant} = GPP * LRU * \frac{[\mathrm{COS}]}{[\mathrm{CO_2}]}, \quad (1)$$

*Corresponding author.
email: thilton@ucmerced.edu
Responsible Editor: Anders Lindroth, Lund University, Sweden.

Tellus B 2015. © 2015 T. W. Hilton et al. This is an Open Access article distributed under the terms of the Creative Commons Attribution 4.0 International License (http://creativecommons.org/licenses/by/4.0/), allowing third parties to copy and redistribute the material in any medium or format and to remix, transform, and build upon the material for any purpose, even commercially, provided the original work is properly cited and states its license.

Citation: Tellus B 2015, **67**, 26329, http://dx.doi.org/10.3402/tellusb.v67.26329

where F_{plant} is the COS uptake by terrestrial plants, GPP is the gross CO_2 uptake by plants, LRU is the normalised leaf-scale relative uptake of COS relative to CO_2, and $[COS]/[CO_2]$ is the ambient ratio of surface concentrations. This GPP-based estimate of the COS plant sink can be used along with other COS source and sink estimates as input to regional and global atmospheric transport models that output atmospheric COS concentrations. Through an inverse analysis, the GPP input can be optimised to achieve the best possible agreement between simulated and observed COS concentrations. An alternative to the use of eq. (1) is a process model which predicts LRU variations with environmental conditions and species (Berry et al., 2013).

For this large-scale COS tracer approach to be effective at constraining GPP, a number of criteria must be met, including:

(1) The relationship between leaf-level CO_2 and COS uptake in eq. (1) must be true. There must be little or no re-emission of COS from the plant, and both species must have little impact on uptake of the other. These criteria have been demonstrated to be true in laboratory studies (Stimler et al., 2010).
(2) The parameters in eq. (1) must also hold constant across plant species and environmental conditions. This has also been demonstrated in laboratory experiments Stimler et al. (2012).
(3) The COS plant uptake must be a dominant source of uncertainty in the transport model relative to other sources and sinks of COS. If this is true we may conclude that transport uncertainty is dominated by the terms of interest to the COS tracer approach, and is not confounded by these other sources and sinks. This criterion is supported by evidence from North American airborne observations (Campbell et al., 2008).
(4) The uncertainties of the LRU and $[COS]/[CO_2]$ parameters in eq. (1) have to be smaller than the uncertainty of GPP. If this criterion is met, the relationship between GPP and COS plant uptake in eq. (1) provides a means to reduce GPP uncertainty by considering COS concentration data. This criterion concerning the relative uncertainties of the parameters in eq. (1) has not been explored. The $[COS]/[CO_2]$ parameter has relatively small uncertainty (Campbell et al., 2008), but an understanding of the relative uncertainties of the GPP and LRU parameters is needed.

Here we focus on criterion 4 above. This LRU criterion is qualitatively consistent with observations of the simultaneous uptake of COS and CO_2 in plant leaves using chamber and eddy flux experiments. The LRU parameter has been measured in plant chamber studies and found to have a stable value of 1.6 ± 0.26 across a range of environmental conditions (Stimler et al., 2012). Field experiments using micrometeorological measurements found similar results with means of 1.3–1.7 (Berkelhammer et al., 2014; Billesbach et al., 2014; Maseyk et al., 2014). The small uncertainty of ground-based LRU measurements suggests the COS tracer approach could be useful for constraining GPP. However, previous work has not explored the COS tracer criterion that uncertainty in LRU must be considerably smaller than GPP uncertainty.

Results from regional and global atmospheric transport simulations have provided a foundation for understanding atmospheric COS variability but they also present results that are potentially inconsistent with chamber-based LRU measurements. Campbell et al. (2008) used a regional atmospheric transport model to find that the observed spatial variation of COS concentrations from the INTEX-NA North American airborne observations (Blake et al., 2008) were consistent with an LRU of approximately 2.2, which is considerably larger than the LRU of 1.6 ± 0.26 from chamber studies. Alternatively, a Northern Hemisphere analysis (Suntharalingam et al., 2008) found the best model performance by doubling the COS plant uptake from Kettle et al. (2002). Kettle et al. (2002) calculated plant uptake based on an LRU value of 1.0 and net primary productivity (NPP) instead of gross primary productivity (GPP). Because GPP is roughly double NPP, the Northern Hemisphere analysis is most consistent with a 1.0 value for LRU which is considerably smaller than the 1.6 ± 0.26 value from chamber studies.

The atmospheric modelling studies of Campbell et al. (2008) and Suntharalingam et al. (2008) each relied on a single ecosystem model estimate of GPP. We hypothesise that this accounts for the divergence in their conclusions. If Campbell et al. (2008) used a relatively low GPP value that could explain their high LRU value. If Suntharalingam et al. (2008) used a relatively high GPP value that could explain their low LRU value. The COS tracer approach hinges on a robust LRU estimate but there has been no work to understand these LRU discrepancies between large-scale atmospheric modelling studies and chamber studies.

Here we explore the criteria for the COS tracer approach that the LRU parameter uncertainty must be smaller than the GPP uncertainty. We compare the chamber-based LRU uncertainty to the uncertainty in GPP suggested by recent model intercomparisons (Huntzinger et al., 2012). We also explore the discrepancies in the LRU from previous atmospheric transport studies and ground-based studies. We analyse the underlying parameters and data used in previous atmospheric modelling studies and we conduct new atmospheric simulations using a mesoscale model (Campbell et al., 2008; Kulkarni et al., 2015) to determine the sensitivity

of simulated COS concentrations to these surface flux parameter inputs. We do not account for the influence of other sources and sinks (criterion 3) because this has been addressed in previous work (Campbell et al., 2008). Rather, our focus is on the fourth criterion which has not been explored at large scales: the relative uncertainty of the terms in eq. (1). While the primary purpose of our transport simulations is to quantify the sensitivity of the simulated COS concentrations relative to the input parameter uncertainty, we also discuss the transport simulation results relative to observed concentration trends which will be the focus of future work.

2. Methods

We test the hypothesis that GPP uncertainty exceeds LRU parameter uncertainty by varying these factors as inputs to the Sulfur Transport and dEposition Model (STEM) (Carmichael et al., 2009; Kulkarni et al., 2015) mesoscale chemical transport model. We simulated transport of COS on a 124 x 124 grid covering most of North America with 60 x 60 km horizontal resolution and 22 vertical levels. The simulations spanned June and July 2008, the peak of the North American growing season. We conducted six STEM runs driven by four different North American GPP estimates and three different LRU estimates, described in detail below.

2.1. Data

2.1.1. Meteorology. We drove the STEM simulations with meteorology from the Weather Research Forecasting version 2.2 (WRFV2-ARW) model. These WRF data were originally produced for the 2008 ARCTAS field campaign (D'Allura et al., 2011). D'Allura et al. (2011) describe the WRF configuration in detail.

2.1.2. GPP. To account for GPP uncertainty we assembled a set of North American GPP model estimates that span the range reported by Huntzinger et al. (2012). For a high GPP estimate we used Can-IBIS (Liu et al., 2005), which incorporates nitrogen cycling into the Integrated BIosphere Simulator (IBIS) (Foley et al., 1996). We used Can-IBIS GPP data for 2004, the most recent year available. For a moderate GPP estimate we used the Carnegie-Ames-Stanford-Approach–Global Fire Emissions Database version 3 (CASA-GFED3) (van der Werf et al., 2010). For a low GPP estimate we used the GPP of Kettle et al. (2002): J. Kettle provided us with the plant surface COS flux data from that study, and we calculated the underlying GPP by noting that they used a modified version of eq. (1), with NPP instead of GPP (GPP = NPP * 2), an LRU of 1.0, and a [COS]/[CO_2] ratio of 1.4 (500 ppt/355 ppm). To allow comparison to Campbell et al. (2008) we also included the GPP of CASA-m15, the earlier version of CASA used by Campbell et al. (2008). The primary difference between CASA-m15 and CASA-GFED3 is that CASA-GFED3 increases GPP in the upper midwestern USA to match crop yield observations. We transformed each GPP estimate from its native grid and resolution to the 124 x 124 STEM grid using the mass-conservative algorithm of the MTXCPLE program of the Models-3/EDSS Input/Output Applications Programming Interface (I/O API) (Coates, 2014). All four of these GPP datasets are available in the supplemental online materials (SOM) for this article. Some are available online; these URLs are listed in the acknowledgements section.

2.2. COS surface flux estimation

To estimate the sensitivity of surface COS concentration ([COS]) to GPP uncertainty we calculated COS plant flux (F_{plant}) from each GPP estimate described in Section 2.1.2 using eq. (1). We used the best-estimate LRU value of 1.61 reported by (Stimler et al., 2012). For the [COS]/[CO_2] ratio we used the average value reported from the INTEX-NA observations of 1.1 (1.1 ± 0.1 ppt COS/ppm CO_2, mean $\pm$ s.d., $n = 440$) (Blake et al., 2008).

To estimate the sensitivity of plant surface COS flux to LRU uncertainty we calculated three F_{plant} estimates using CASA-GFED3 GPP and eq. (1). We used the same [COS]/[CO_2] ratio of 1.1 ppt COS/ppm CO_2, and three LRU values: 1.35, 1.61 and 1.87. These three LRU values span the range of 1.61 ± 0.26 reported by Stimler et al. (2012). Stimler et al. (2011) note that C3 plants exhibit a larger LRU (1.82 ± 0.18) than C4 plants (1.16 ± 0.20), and that LRU can increase substantially under low light conditions ($< 191 \mu$ mol photon m^{-2} s^{-1}). To investigate these LRU uncertainties we considered two additional F_{plant} estimates using the Simple Biosphere Model (SiB) (Sellers et al., 1996; Baker et al., 2008, 2010). The first used the same approach outlined above: F_{plant} was estimated using SiB GPP and eq. (1), with the [COS]/[CO_2] ratio of 1.1 ppt COS/ppm CO_2, and LRU of 1.61. The second used SiB's mechanistically-calculated F_{plant} estimate that considers light conditions, photosynthetic pathways and soil fluxes. This helps us to quantify the uncertainty caused by using a prescribed LRU value.

We did not simulate the effect of the uncertainty of the [COS]/[CO_2] parameter because it is considerably smaller than the uncertainty of both LRU and GPP (Campbell et al., 2008, supporting online material; based on the observations below 1 km above sea level). However, we did examine how assumptions regarding this ratio influenced previous regional and global simulations (Campbell et al., 2008; Suntharalingam et al., 2008).

This produced six F_{plant} estimates, summarised in Table 1 and Fig. 2. We supplied each F_{plant} estimate (Fig. 2, second row) as driver data to a unique STEM run. The resulting six simulated surface COS concentration fields (Fig. 2, third row) are the basis of our analyses.

3. Results and discussion

We found that the single estimates of GPP used in previous atmospheric modelling studies could explain their good models–observation agreement despite their use of LRU parameter estimates that are outside the range found by subsequent chamber and eddy flux studies. The GPP and LRU estimates for the regional and global modelling studies are plotted in Fig. 1 (points) along with the range of possible values (lines). Campbell et al. (2008) used an LRU value of 2.2 for the North American growing seasons which is larger than the 1.6 ± 0.26 range suggested by chamber measurements. Campbell et al. (2008) used a GPP estimate from a version of the CASA model (CASA-m15) that had nearly the lowest GPP for the INTEX-NA domain (midwestern and eastern U.S. region) of all the models we identified for this region. The same COS plant uptake could be obtained with eq. (1) by lowering the LRU estimate by 15%, to within the chamber-based range, and increasing the GPP flux by 17.6%. This larger GPP would still be well within the range of possible GPP values for the North American INTEX-NA domain. The results of Suntharalingam et al. (2008) are consistent with an LRU of 1.0 which is smaller than the 1.6 ± 0.26 range suggested by chamber measurements. This Northern Hemisphere analysis used a GPP estimate that had the highest GPP of all the models we identified for this domain. The same COS plant uptake could be obtained with eq. (1) by increasing the LRU estimate by 34%, to within the chamber-based range, and decreasing the GPP flux by 25.3%. This smaller GPP would still be well within the range of possible GPP values for the Northern Hemisphere. We also note that the Northern Hemisphere analysis used a flux that was based on a relatively large $[COS]/[CO_2]$ ratio from background concentrations rather than the relatively low values observed in the continental boundary layer (Campbell et al., 2008). If the lower boundary layer ratio is used, the GPP must be lowered only 6% to accommodate an LRU of 1.35.

Table 1. Input used to drive the six STEM runs described in Section 2.2

GPP model	July–Aug full-domain GPP (pg C)	LRU
Can-IBIS	9.30	1.61
CASA-m15	5.76	1.61
Kettle	5.77	1.61
CASA-GFED3	6.12	1.61
CASA-GFED3	6.12	1.35
CASA-GFED3	6.12	1.87

The GPP and LRU values below were fed as inputs to eq. (1) to calculate COS surface plant flux (F_{plant}). F_{plant} was then used to drive STEM. $[COS]/[CO_2]$ was set to 1.1 based on INTEX-NA observations (Blake et al., 2008) for all STEM runs.

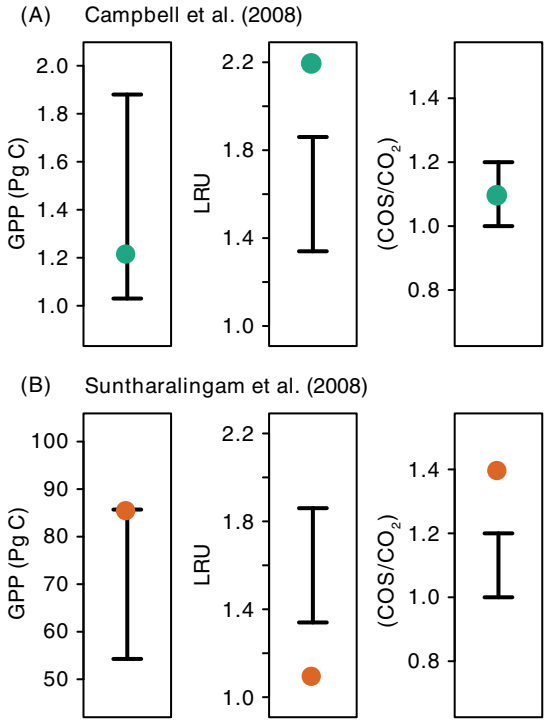

Fig. 1. COS plant flux parameters used in previous atmospheric modelling studies (points) and the range of possible parameters (lines). Two atmospheric COS modelling studies have been reported including a study of the Midwestern and Eastern U.S. growing season (top row; Campbell et al., 2008) and the Northern Hemisphere seasonal variation (bottom row; Suntharalingam et al., 2008). Line widths are the range of model input based on ecosystem model variability for GPP, ground-based experiments for LRU and atmospheric observations for $[COS]/[CO_2]$.

The uncertainty of the flux parameters in Fig. 1 (lengths of boxes) can also be used to consider the COS tracer criteria that the uncertainty for GPP must be considerably larger than the uncertainty in LRU and $[COS]/[CO_2]$. Chamber-based experiments have found a relatively robust value of LRU of 1.6 ± 0.26 across a range of environmental conditions (Stimler et al., 2012). This LRU uncertainty of 15% is considerably lower than the GPP uncertainty that is reflected in the large spread of large-scale ecosystem model estimates (Huntzinger et al., 2012). The set of ecosystem models we considered here have a model-to-model uncertainty of 46 and 23% for the North American INTEX-NA and Northern Hemisphere domains, respectively. The uncertainty in $[COS]/[CO_2]$ is only 9% (Campbell et al., 2008, supporting

online material; based on the observations below 1 km above sea level).

Next we used the uncertainty in GPP and LRU to generate a range of COS plant flux estimates with eq. (1) and used these fluxes as input to the STEM regional transport model as described in Section 2.2. Figure 2 maps the input fluxes (first and second row) as well as the concentration output as the vertical drawdown (difference between free troposphere and boundary layer concentrations, third row).

The modelled vertical drawdown for the atmospheric simulations shows the propagation of uncertainty associated with the LRU and GPP parameters mapped in Fig. 2. Among the four GPP simulations (columns 1–4) the difference between the vertical drawdown for different simulations at a given time and location ranges from 0 ppt (mostly in the semi-arid western USA) to 166 ppt, with a median of 6.8 ppt and a standard deviation of 16.4 ppt. Among the three LRU simulations (columns 4–6) the difference between the vertical drawdown for different simulations at a given time and location ranges from 0 ppt to 41 ppt, with a median of 2.5 ppt and standard deviation of 5.7 ppt. The ratios of medians (6.8/2.5) and standard deviations (16.4/5.7) correspond to the ratio of LRU uncertainty to GPP uncertainty (46%/15%).

Figure 3 compares STEM COS vertical drawdown driven by SiB GPP and eq. (1) with [COS]/[CO_2] ratio of 1.1 ppt COS/ppm CO_2, and LRU of 1.61 (left panel) to STEM COS vertical drawdown driven by SiB's mechanistic F_{plant} (centre panel). We found that the mechanistic F_{plant} results in a simulated vertical drawdown 10–30% larger than the prescribed LRU F_{plant} (right panel) across most of the USA and Canada. The mean difference is $+1.5$ ppt, with a standard deviation of 1.6 ppt. This is consistent with the LRU range of $\pm 15\%$ (1.61 ± 0.26) found by Stimler et al. (2012). This suggests that the uncertainty contributed by using a prescribed LRU rather than a mechanistic plant flux is much smaller than the GPP uncertainty.

Figure 4 shows the distribution of daily ratios of (drawdown spread among the GPP runs) to (drawdown spread among the LRU runs). All of the medians are between 2.4 and 3.4, also consistent with the ratio of GPP uncertainty to LRU uncertainty (46%/15%).

We found that Campbell et al. (2008) found a good agreement with observations despite an overestimated LRU because it used a small GPP from the CASA-m15 model. More recent versions of the CASA model (e.g. CASA-GFED3) have been calibrated with midwestern USA crop yields and have a GPP that is roughly 45% larger over the midwestern and eastern U.S. region where the INTEX-NA flights occurred. This upward revision is also supported by recent results from remotely sensed fluorescence which indicates that most ecosystem models underestimate GPP in the midwest U.S. region (Guanter et al., 2014).

While the purpose of this analysis is to examine model sensitivity we also note that the mean over-land drawdown across all six STEM runs of 22 ppt is roughly consistent with

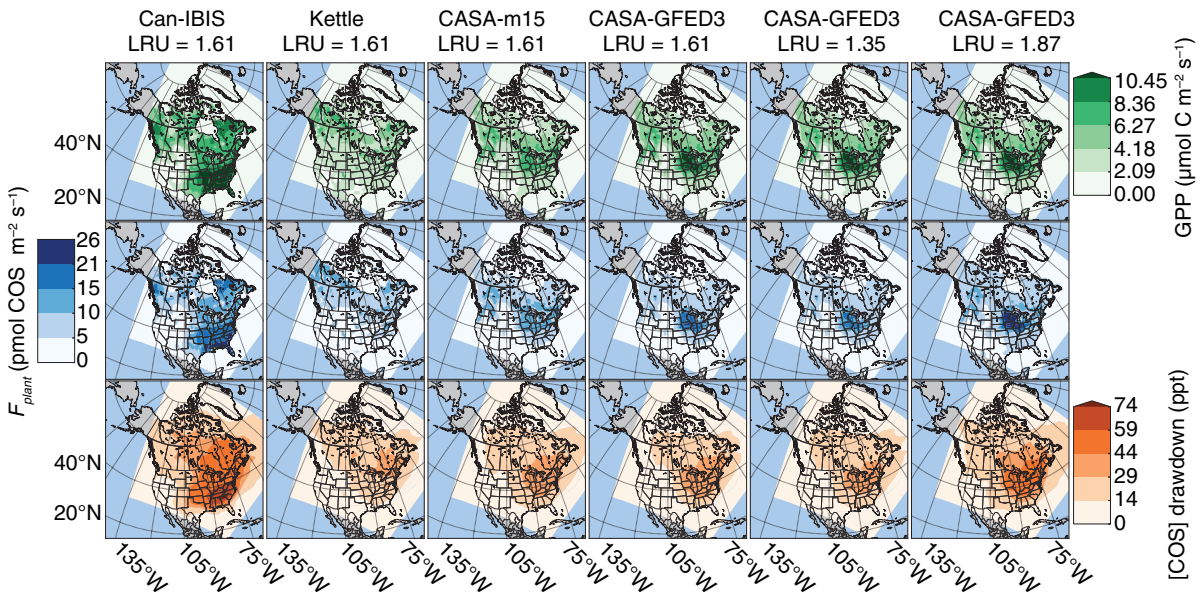

Fig. 2. First row: July and August mean gross primary productivity (GPP). Second row: July and August mean COS plant flux (F_{plant}). Third row: July and August mean COS vertical drawdown. F_{plant} was calculated from GPP by eq. (1) and passed as a driver to STEM. Vertical drawdown was simulated by STEM; it is the decrease in COS concentration between the surface and the upper atmosphere due to plant uptake. The six STEM runs (columns) are described in Section 2.2 and Table 1.

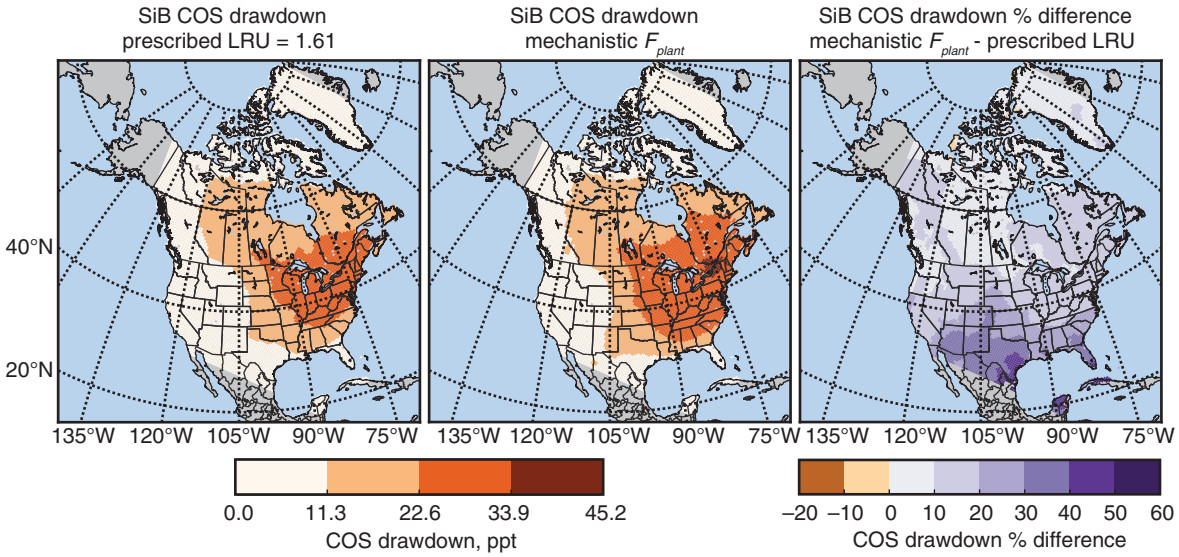

Fig. 3. STEM COS vertical drawdown driven by SiB COS plant fluxes. In the left panel SiB F_{plant} was calculated from SiB GPP by eq. (1) using LRU = 1.61. In the centre panel F_{plant} was calculated using SiB's mechanistic F_{plant}. The right panel shows the percent difference. The difference ranges from 0 to 30% over almost all of the United States and Canada; this is consistent with the roughly 30% (1.61 ± 0.26) LRU range of Stimler et al. (2012). The absolute vertical drawdown difference (not shown) ranges from −0.3 to 7.0 ppt.

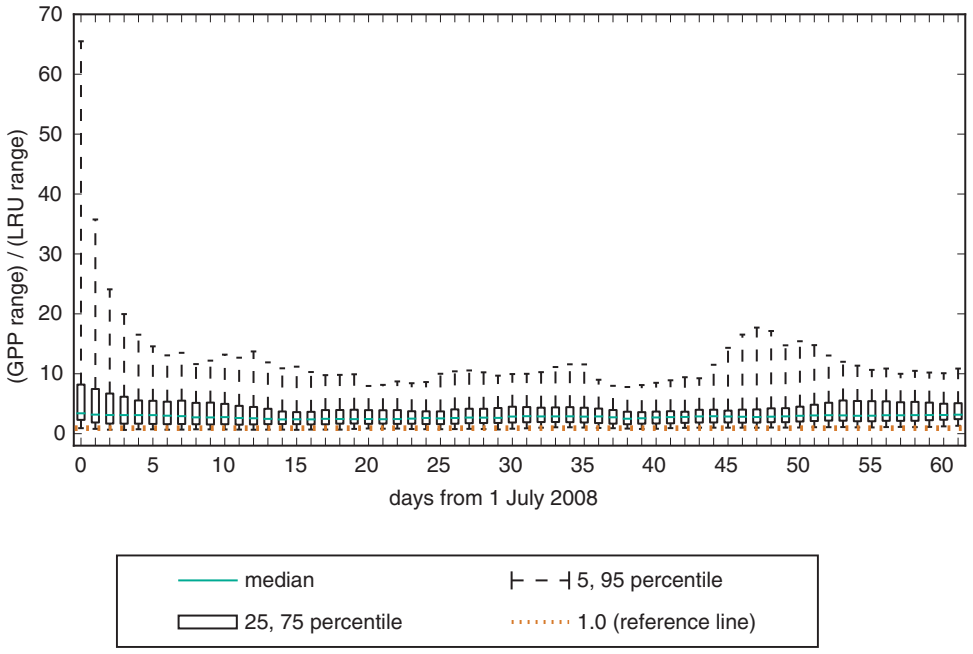

Fig. 4. Box and whisker plots showing the relative sensitivities of simulated COS vertical drawdown to uncertainty in leaf relative uptake (LRU) and gross primary productivity (GPP). Vertical drawdown is the imposed background COS concentration of 450 ppt minus the STEM-simulated surface COS concentration. Ratios are (GPP range)/(LRU range). GPP range and LRU range were calculated from mid-day mean COS vertical drawdown. GPP range is maximum minus minimum drawdown among the four GPP-varying runs (Can-IBIS, Kettle, CASA-m15, CASA-GFED3). LRU range is the maximum minus minimum drawdown among the three LRU-varying runs (CASA-GFED3 LRU = 1.35, CASA-GFED3 LRU = 1.61, CASA-GFED3 LRU = 1.87). STEM runs are described in Section 2.2 and Table 1. Each box and whisker plot summarises 1 d mid-day mean drawdown for all STEM grid cells. Almost all of the ratios are greater than 1.0 and all medians are between 2.4 and 3.4. This suggests that GPP uncertainty consistently produces more [COS] variability than LRU uncertainty by a factor of roughly 3.

the low end of the observed drawdown ranges at NOAA airborne observation sites in Wisconsin, USA (54 ± 30 ppt) and Iowa, USA (51 ± 28 ppt). A robust quantitative comparison of modelled drawdown to observed drawdown would require more sophisticated interpolation of gridded model results to the observation locations. This is beyond the scope of the present study. However we believe the rough agreement of magnitudes lends credibility to the model results. The rough model–observation agreement is consistent with previous work that shows that the plant flux is the dominant source of variability for the North American growing season relative to boundary conditions and other surface fluxes (Campbell et al., 2008). However future work that focuses on atmospheric inversion in addition to model sensitivity will need to account for these other sources of variability. In particular, recent eddy flux and chamber observations show evidence of night plant uptake that is not related to GPP and a soil source, both of which need to be parameterised in flux models and examined in atmospheric transport simulations (Billesbach et al., 2014; Maseyk et al., 2014; White et al., 2010).

4. Conclusions

The COS tracer approach [eq. (1)] to quantifying GPP depends on the underpinning criterion that uncertainty in GPP is smaller than uncertainty in LRU. Here we have demonstrated that vertical drawdown of COS is much more sensitive to GPP uncertainty than to LRU uncertainty, and therefore that this important criterion is satisfied. We have also demonstrated that the wide range of LRU values found by previous atmospheric modelling studies (relative to plant-based chamber studies) can be explained by the relatively large uncertainty in North American GPP estimates. Both of these results are encouraging for the viability of the COS tracer approach to diagnosing GPP. Further work is needed to confirm that modelled COS concentrations are consistent with airborne observations and to examine other sources of COS concentration variability.

5. Acknowledgements

G. J. Collatz and S. R. Kawa provided CASA-m15 GPP data. J. Kettle provided surface plant COS flux data from Kettle et al. (2002). S. A. Montzka and C. Sweeney provided airborne and ground-based COS observations. CASA-GFED3 GPP data were obtained from the North American Carbon Program (www.nacp-files.nacarbon.org/nacp-kawa-01/, last accessed 22 July 2014). I. Baker provided SiB CO_2 GPP and COS GPP data. A. D'Allura helped to set up the WRF runs that drove our STEM simulations. K. Laird and N. Graves, of the UC Merced School of Engineering, worked hard on short notice to set up a data processing machine to conduct our SiB experiments when our main processing platform suffered critical hardware failures during the revision phase; we could not have submitted timely revisions without this help. Data pre- and post-processing was performed using SciPy (Jones et al., 2001) and matplotlib (Hunter, 2007).

References

Arneth, A., Harrison, S. P., Zaehle, S., Tsigaridis, K., Menon, S. and co-authors. 2010. Terrestrial biogeochemical feedbacks in the climate system. *Nat. Geosci.* **3**(8), 525–532. DOI: 10.1038/ngeo905.

Asaf, D., Rotenberg, E., Tatarinov, F., Dicken, U., Montzka, S. A. and co-authors. 2013. Ecosystem photosynthesis inferred from measurements of carbonyl sulphide flux. *Nat. Geosci.* **6**(3), 186–190. DOI: 10.1038/ngeo1730.

Baker, I. T., Denning, A. S. and Stöckli, R. 2010. North American gross primary productivity: regional characterization and interannual variability. *Tellus B.* **62**(5), 533–549. DOI: 10.1111/j.1600-0889.2010.00492.x.

Baker, I. T., Prihodko, L., Denning, A. S., Goulden, M., Miller, S. and co-authors. 2008. Seasonal drought stress in the Amazon: reconciling models and observations. *J. Geophys. Res. Biogeosci.* **113**(G00B01). DOI: 10.1029/2007JG000644.

Beer, C., Reichstein, M., Tomelleri, E., Ciais, P., Jung, M. and co-authors. 2010. Terrestrial gross carbon dioxide uptake: global distribution and covariation with climate. *Science.* **329**, 834–838. DOI: 10.1126/science.1184984.

Berkelhammer, M., Asaf, D., Still, C., Montzka, S., Noone, D. and co-authors. 2014. Constraining surface carbon fluxes using in situ measurements of carbonyl sulfide and carbon dioxide. *Glob. Biogeochem. Cycles.* **28**(2), 161–179. DOI: 10.1002/2013GB004644.

Berry, J., Wolf, A., Campbell, J. E., Baker, I., Blake, N. and co-authors. 2013. A coupled model of the global cycles of carbonyl sulfide and CO_2: a possible new window on the carbon cycle. *J. Geophys. Res. Biogeosci.* **118**(2), 842–852. DOI: 10.1002/jgrg.20068.

Billesbach, D., Berry, J., Seibt, U., Maseyk, K., Torn, M. and co-authors. 2014. Growing season eddy covariance measurements of carbonyl sulfide and {CO_2} fluxes: {COS} and {CO2} relationships in southern great plains winter wheat. *Agri. Forest Meteorol.* **184**, 48–55. DOI: 10.1016/j.agrformet.2013.06.007.

Blake, N. J., Campbell, J. E., Vay, S. A., Fuelberg, H. E., Huey, L. G. and co-authors. 2008. Carbonyl sulfide (OCS): large-scale distributions over North America during INTEX-NA and relationship to CO_2. *J. Geophys. Res. Atmos.* **113**(D09S90). DOI: 10.1029/2007JD009163.

Blake, N. J., Streets, D. G., Woo, J.-H., Simpson, I. J., Green, J. and co-authors. 2004. Carbonyl sulfide and carbon disulfide: large-scale distributions over the western Pacific and emissions from Asia during TRACE-P. *J. Geophys. Res. Atmos.* **109**(D15S05). DOI: 10.1029/2003JD004259.

Blonquist, J. M., Montzka, S. A., Munger, J. W., Yakir, D., Desai, A. R. and co-authors. 2011. The potential of carbonyl sulfide as a proxy for gross primary production at flux tower sites.

J. Geophys. Res. Biogeosci. **116**(G04019). DOI: 10.1029/2011JG001723.

Campbell, J. E., Carmichael, G. R., Chai, T., Mena-Carrasco, M., Tang, Y. and co-authors. 2008. Photosynthetic control of atmospheric carbonyl sulfide during the growing season. *Science*. **322**(5904), 1085–1088. DOI: 10.1126/science.1164015.

Carmichael, G. R., Adhikary, B., Kulkarni, S. DAllura, A., Tang, Y. and co-authors. 2009. Asian aerosols: current and year 2030 distributions and implications to human health and regional climate change. *Environ. Sci. Technol.* **43**(15), 5811–5817. DOI: 10.1021/es8036803.

Coates, C. J., Jr. 2014. *The BAMS/EDSS/Models-3 I/O API: user manual*. UNC Institute for the Environment, Environmental Modeling Center, Raleigh, NC. Online at: http://www.cmascenter.org/ioapi/

Commane, R., Herndon, S. C., Zahniser, M. S., Lerner, B. M., McManus, J. B. and co-authors. 2013. Carbonyl sulfide in the planetary boundary layer: coastal and continental influences. *J. Geophys. Res. Atmos.* **118**(14), 8001–8009. DOI: 10.1002/jgrd.50581.

D'Allura, A., Kulkarni, S., Carmichael, G. R., Finardi, S., Adhikary, B. and co-authors. 2011. Meteorological and air quality forecasting using the WRF–STEM model during the 2008 ARCTAS field campaign. *Atmos. Environ.* **45**(38), 6901–6910. DOI: 10.1016/j.atmosenv.2011.02.073.

Fisher, J. B., Sikka, M., Oechel, W. C., Huntzinger, D. N., Melton, J. R. and co-authors. 2014. Carbon cycle uncertainty in the Alaskan Arctic. *Biogeosci. Discuss.* **11**(2), 2887–2932. DOI: 10.5194/bgd-11-2887-2014.

Foley, J. A., Prentice, I. C., Ramankutty, N., Levis, S., Pollard, D. and co-authors. 1996. An integrated biosphere model of land surface processes, terrestrial carbon balance, and vegetation dynamics. *Glob. Biogeochem. Cycles*. **10**(4), 603–628. DOI: 10.1029/96GB02692.

Friedlingstein, P., Cox, P., Betts, R., Bopp, L., von Bloh, W. and co-authors. 2006. Climate-carbon cycle feedback analysis: results from the C[4]MIP model intercomparison. *J. Clim.* **19**(14), 3337–3353. DOI: 10.1175/JCLI3800.1.

Friedlingstein, P., Meinshausen, M., Arora, V. K., Jones, C. D., Anav, A. and co-authors. 2014. Uncertainties in CMIP5 climate projections due to carbon cycle feedbacks. *J. Clim.* **27**(2), 511–526. DOI: 10.1175/JCLI-D-12-00579.1.

Guanter, L., Zhang, Y., Jung, M., Joiner, J., Voigt, M. and co-authors. 2014. Global and time-resolved monitoring of crop photosynthesis with chlorophyll fluorescence. *Proc. Natl. Acad. Sci. USA*. **111**, E1327–E1333. DOI: 10.1073/pnas.1320008111.

Hunter, J. D. 2007. Matplotlib: a 2d graphics environment. *Comput. Sci. Eng.* **9**(3), 90–95.

Huntzinger, D., Post, W., Wei, Y., Michalak, A., West, T. and co-authors. 2012. North American Carbon Program (NACP) regional interim synthesis: terrestrial biospheric model intercomparison. *Ecol. Model.* **232**, 144–157. DOI: 10.1016/j.ecolmodel.2012.02.004.

Jones, E., Oliphant, T., Peterson, P. and others. 2001. SciPy: open source scientific tools for Python. Online at: http://www.scipy.org/

Kettle, A. J., Kuhn, U., von Hobe, M., Kesselmeier, J. and Andreae, M. O. 2002. Global budget of atmospheric carbonyl sulfide: temporal and spatial variations of the dominant sources and sinks. *J. Geophys. Res. Atmos.* **107**(D22), ACH 25–1–CH 25–16. DOI: 10.1029/2002JD002187.

Kuai, L., Worden, J., Kulawik, S. S., Montzka, S. A. and Liu, J. 2014. Characterization of Aura TES carbonyl sulfide retrievals over ocean. *Atmos. Meas. Tech.* **7**(1), 163–172. DOI: 10.5194/amt-7-163-2014.

Kulkarni, S., Sobhani, N., Miller-Schulze, J. P., Shafer, M. M., Schauer, J. J. and co-authors. 2015. Source sector and region contributions to BC and $PM^{2.5}$ in Central Asia. *Atmos. Chem. Phys.* **15**(4), 1683–1705. DOI: 10.5194/acp-15-1683-2015.

Liu, J., Price, D. T. and Chen, J. M. 2005. Nitrogen controls on ecosystem carbon sequestration: a model implementation and application to Saskatchewan, Canada. *Ecol. Model.* **186**(2), 178–195. DOI: 10.1016/j.ecolmodel.2005.01.036.

Maseyk, K., Berry, J. A., Billesbach, D., Campbell, J. E., Torn, M. S. and co-authors. 2014. Sources and sinks of carbonyl sulfide in an agricultural field in the Southern Great Plains. *Proc. Natl. Acad. Sci. USA*. **111**(25), 9064–9069. DOI: 10.1073/pnas.1319132111.

Montzka, S. A., Calvert, P., Hall, B. D., Elkins, J. W., Conway, T. J. and co-authors. 2007. On the global distribution, seasonality, and budget of atmospheric carbonyl sulfide (COS) and some similarities to CO_2. *J. Geophys. Res. Atmos.* **112**(D09302). DOI: 10.1029/2006JD007665.

Sellers, P. J., Randall, D. A., Collatz, G. J., Berry, J. A., Field, C. B. and co-authors. 1996. A revised land surface parameterization (SiB2) for atmospheric GCMS. Part I: model formulation. *J. Clim.* **9**, 676–705.

Stimler, K., Berry, J. A., Montzka, S. A. and Yakir, D. 2011. Association between carbonyl sulfide uptake and $^{18}\Delta$ during gas exchange in C_3 and C_4 leaves. *Plant Physiol.* **157**(1), 509–517. DOI: 10.1104/pp.111.176578.

Stimler, K., Berry, J. A. and Yakir, D. 2012. Effects of carbonyl sulfide and carbonic anhydrase on stomatal conductance. *Plant Physiol.* **158**(1), 524–530. DOI: 10.1104/pp.111.185926.

Stimler, K., Montzka, S. A., Berry, J. A., Rudich, Y. and Yakir, D. 2010. Relationships between carbonyl sulfide (COS) and CO_2 during leaf gas exchange. *New Phytolog.* **186**(4), 869–878. DOI: 10.1111/j.1469-8137.2010.03218.x.

Suntharalingam, P., Kettle, A. J., Montzka, S. M. and Jacob, D. J. 2008. Global 3-D model analysis of the seasonal cycle of atmospheric carbonyl sulfide: implications for terrestrial vegetation uptake. *Geophys. Res. Lett.* **35**(L19801), 1–6. DOI: 10.1029/2008GL034332.

van der Werf, G. R., Randerson, J. T., Giglio, L., Collatz, G. J., Mu, M. and co-authors. 2010. Global fire emissions and the contribution of deforestation, savanna, forest, agricultural, and peat fires (1997–2009). *Atmos. Chem. Phys.* **10**(23), 11707–11735. DOI: 10.5194/acp-10-11707-2010.

Welp, L. R., Keeling, R. F., Meijer, H. A. J., Bollenbacher, A. F., Piper, S. C. and co-authors. 2011. Interannual variability in the oxygen isotopes of atmospheric CO_2 driven by El Niño. *Nature*. **477**(7366), 579–582. DOI: 10.1038/nature10421.

White, M. L., Zhou, Y., Russo, R. S., Mao, H., Talbot, R. and co-authors. 2010. Carbonyl sulfide exchange in a temperate loblolly pine forest grown under ambient and elevated CO_2. *Atmos. Chem. Phys.* **10**(2), 547–561. DOI: 10.5194/acp-10-547-2010.